Comparison of THOR-50M-RS to PMHS in Upright Frontal Sled Impacts

Mary K. Gallaher, John-Paul Donlon, Logan M. Mann, Reagan T. Hollar,
Isabella L. Nazari, Ayush P. Mehta, Jason L. Forman

Abstract This study aimed to compare the THOR-50M-RS to previously published tests with mid-size male post-mortem human subjects (PMHS) in upright, frontal sled impacts. The test condition was a full-frontal 30 km/h impact with a reinforced production seat, a footpan, and a production-style restraint with retractor pretensioner and integrated force limiter. Three tests were run with the THOR-50M-RS to compare to tests with three mid-size male PMHS. Similar overall occupant kinematics were seen across tests with PMHS and THOR-50M-RS. The PMHS experienced higher belt forces in the shoulder and lap belts. Entrapment of the shoulder belt in the gap between the neck assembly and shoulder cover of the THOR-50M-RS occurred in all three tests. Pelvis restraint by the lap belt and seat differed among PMHS and between PMHS and the THOR-50M-RS. Submarining occurred in one of the three PMHS tests. There was no evidence of submarining in the tests with the THOR-50M-RS. More rearward angular displacement of the pelvis was observed in the case of the THOR-50M-RS. Overall, the THOR-50M-RS had a similar overall kinematic response, with some differences in belt forces, shoulder belt engagement, and pelvis rotation.

Keywords Frontal Impact, THOR-50M-RS, Biofidelity, Restraint, Upright

I. INTRODUCTION

Anthropomorphic Test Devices (ATDs) are utilised heavily in the automotive industry as surrogates for human occupants in regulatory testing and assessment of vehicle safety features [1]. In order to effectively protect occupants in road collisions, assessment of safety features must use tools that behave similarly to human occupants, a term coined as biofidelity. The Test device for Human Occupant Restraint 50th percentile male (THOR-50M) is an example of an ATD used in impact testing that has been evaluated for its biofidelity in the past [2]. Whole-body evaluation of the THOR-50M included a variety of restraint conditions, namely Gold Standard 1 (GS1), Gold Standard 2 (GS2), Gold Standard 3 (GS3), and Far-Side Frontal Oblique (FSFO). These conditions cover a spectrum of simplified restraint, from a rigid shoulder belt and simplified seat in GS1, a force limited belt and simplified seat in GS2 and GS3, to a car-like environment featuring a front-passenger air bag and knee bolster in FSFO [2-5]. Another study evaluated the biofidelity of the THOR-50M in a vehicle environment using a full vehicle seat, knee bolster, and steering wheel [6]. Some biofidelity assessments of the THOR-50M have also been conducted in reclined seating postures, but also with simplified seating configurations, like the semi-rigid seat [7], and in rear impacts [8].

Proper pelvis restraint is axiomatic for restraint biomechanics [9]. Primary restraint of the pelvis is delivered by the seat and the lap belt. Pelvis biofidelity is important for ATDs to appropriately capture lap-belt restraint. This is highlighted by comparison of the THOR-50M to post-mortem human subjects (PMHS) in recline. Shin *et al.* found that the pelvis of the THOR-50M rotated in the opposite direction of PMHS in a condition with a simplified seat and production-style prototype restraint [7]. These observed differences in pelvis rotation motivated modifications to the ATD reflected in the THOR-50M-Reclined Seating (THOR-50M-RS) [10]. The THOR-50M-RS is a modified version of the THOR-50M that was created to increase its range of usability to reclined seating environments. Changes were made to the abdomen, spine, pelvis, and sacrum of the THOR-50M-RS to aid in reclining of the device. However, even though the modifications were designed to increase the range of usability to reclined postures, it is still the goal that the ATD is also usable in upright seating postures. The biofidelity of the THOR-50M-RS has only been assessed in three reclined conditions utilising a semi-rigid seat and different knee bolster designs[11], while the THOR-50M has been assessed in range of simplified and realistic vehicle-like conditions[2], demonstrating a need for the THOR-50M-RS to be evaluated in a simplified upright frontal test like the simplified Gold Standard conditions; in addition to more realistic seating and restraint configurations.

M. K. Gallaher (e-mail: gallaher@virginia.edu; tel: +1-434-982-4169) is a PhD student in Mechanical and Aerospace Engineering, J-P. Donlon is senior research specialist, L. M. Mann is an undergraduate researcher, R. T. Hollar is an intermediate research specialist, I. L. Nazari and A. P. Mehta are PhD students, and J. L. Forman is an Associate Professor of Mechanical and Aerospace Engineering, all at the University of Virginia Center for Applied Biomechanics, Charlottesville, Virginia, USA.

Donlon et al. performed a series PMHS tests examining occupant motions during pre- crash vehicle accelerations [12]. As a part of that investigation, three tests were performed with subjects in an upright nominal position, with a prototype production-style seat belt, production seat bottom, and no knee restraint. Occupant kinematics of the PMHS and boundary loads, including the seat belt and the seat, were measured. This seating and restraint configuration meets the need for a frontal biofidelity assessment condition of intermediate complexity.

The goal of this study was to compare the THOR-50M-RS to previously published tests of mid-size male PMHS in an upright frontal sled impact with a production seat and seat-belt system [12].

II. METHODS

Three tests were performed with the THOR-50M-RS in a frontal impact condition with a production-style seat and seat belt and compared to previously published tests of mid-size male PMHS in the same condition (Table I) [12]. A Seattle Safety reverse acceleration servo sled (1.4 MN ServoSled®, Seattle Safety, Auburn, WA, USA) was used in these impacts to achieve a delta-V of 30 km/h and a 9 G trapezoidal acceleration (Fig. 1) [4].

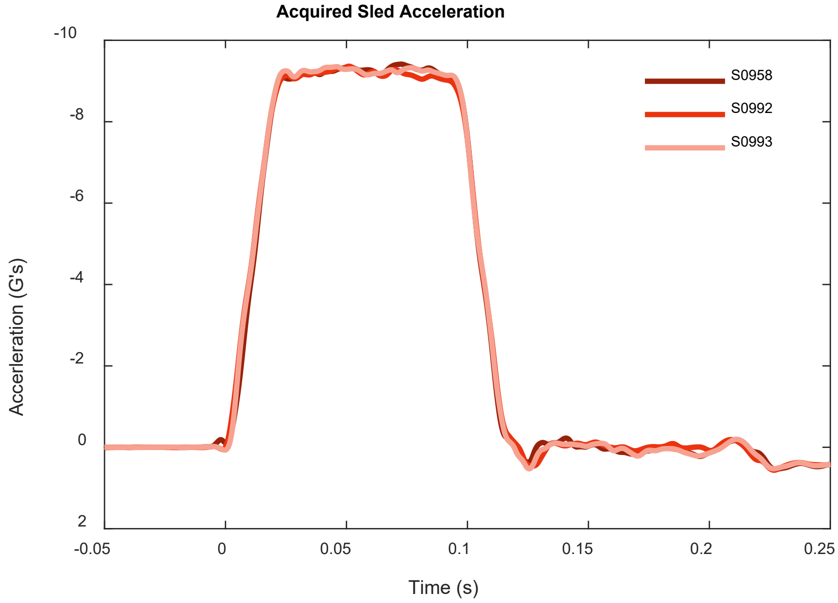

Fig. 1. Acquired sled accelerations from the tests with the THOR-50M-RS.

TABLE I
TEST MATRIX

UVA Test No.	Occupant Type	Height (cm)	Mass (kg)	Delta – V (km/h)	Restraint Type	NHTSA BioDB No.
UVAS0500*	50th %ile male PMHS	182	72	30	3-pt belt	-
UVAS0503*	50th %ile male PMHS	178	73	30	3-pt belt	-
UVAS0506*	50th %ile male PMHS	175	82	30	3-pt belt	-
UVAS0958	THOR-50M-RS	172	77	30	3-pt belt	b15707
UVAS0992	THOR-50M-RS	172	77	30	3-pt belt	b15708
UVAS0993	THOR-50M-RS	172	77	30	3-pt belt	b15709

**PMHS data reproduced from [12].*

Test Environment

A buck featuring a seat, footpan, and 3-point seat belt was used (Fig. 2). The occupants were seated on a reinforced production-style seat from the second row of a 2017 Toyota Sienna (captain's chair-style seat). The feet of the occupant were secured by rubber-padded metal clamps in a footpan consisting of a pair of aluminum channels. A custom, non-production 3-point seat-belt system with integrated retractor pre-tensioner (B1) and nominal 2 kN load limiter was used (Joyson Safety Systems, Auburn Hills, MI). The retractor pre-tensioner was fired at 10 ms post-time zero of the impact.

Fig. 2. Left: test fixture featuring a representative mid-size male PMHS (S0503). Right: test fixture featuring THOR-50M-RS (S0992).

Subject and Belt Positioning

Positioning targets for the THOR-50M-RS were derived from the tests with mid-size male PMHS [12]. Due to differences in stature (Table I), priority targets were the H-Point location, femur angle, and gross torso posture (Table II and Appendix A, Fig. A1). The buckle and lap-belt anchor locations with respect to the seat approximated the restraint configuration of a mid-size passenger vehicle, and the lap belt was routed as low as possible across the lap while remaining fully on the pelvis flesh of the ATD (Appendix A, Fig. A2). The seat belt was positioned such that the shoulder belt crossed the ATD at mid-clavicle and mid-sternum, achieving a frontal angle of the belt of 52 degrees, measured with respect to the horizontal with a protractor where the shoulder belt crossed the centreline of the ATD (Appendix A, Fig. A1). The D-Ring assembly height was adjusted to achieve a target shoulder-belt take-off angle of 30 degrees, measured with respect to the horizontal from the shoulder of the occupant to the centre of the belt at the D-Ring (Appendix A, Fig. A1).

TABLE II
THOR-50M-RS POSITIONING TARGETS AND MEASUREMENTS

Measurement	PMHS Avg.	THOR Target	S0958	S0992	S0993
H-Point (left)		*0*	0	0	2
Femur Angle (avg.)+	*18.5*	*18*	17.5	18	18
Tibia Angle (avg.)+	*53*	*42*	41	42	41.5
Torso Angle*	*10**	*60*	60	60	60
Frontal Seat-belt Angle	*52*	*52*	51	52	52
Shoulder-belt Take-off Angle	*28*	*30*	30	30	30

**Torso angle for the PMHS was measured on the posterior aspect of the subject between the motion-tracking arrays at the T1 and L2 locations relative to the vertical. During the first test with the THOR-50M-RS, the posterior approximation was used to define a similar target using a measurement between the acromion and H-Point of the THOR-50M-RS relative to the horizontal.*
+Femur angles were measured from the H-point (greater trochanter) to the knee joint (lateral condyle). Tibia angles were measured from the knee joint (lateral condyle) to the ankle joint (lateral malleolus).

Instrumentation

Instrumentation data were collected at 10,000 Hz and motion-capture data were collected at 1,000 Hz from 50 ms before time zero until at least 300 ms after time zero. High-speed videos were also captured from three off-board cameras recording at 1,000 frames per second. Seat forces and moments were measured by a load cell mounted at the base of the seat. Forces and moments were also measured in a load cell in the footpan. Seat-belt tension gauges were attached along the belt at the upper shoulder belt (between the D-ring and the shoulder), lower shoulder belt (between the chest and the sliding latch-plate) and lap belt (between the lap and the anchor). The THOR-50M-RS was instrumented with 3D motion-tracking arrays to track occupant kinematics. The locations of the mounts on the THOR-50M-RS were attached to each rigid segment of the spine: head, upper thoracic spine, lower thoracic spine, upper lumber spine, and pelvis. In the PMHS tests in the same condition, the subjects were instrumented with motion-tracking arrays at the head, T1, T8, and L2 vertebrae, and the pelvis. Coordinate systems and instrumentation were configured and analysed in accordance with recommendations by the Society of Automotive Engineers J211 [13]. In addition to motion capture, accelerometers, angular rate sensors, load cells, and deflection sensors built into the ATD measured forces, moments, and deflections at measurement points throughout the ATD (data available upon request or via the NHTSA Biomechanics Database, Test No. 15707-15709 [14]).

Kinematic Analysis

Local coordinate systems were defined for the anatomic locations of the PMHS and the marker arrays were transformed to track the motion of the anatomic structures during the impact. For the THOR-50M-RS, the local coordinate systems for each rigid segment of the spine (upper T-spine, lower T-spine, and upper L-spine) were defined. Using the method from Parent *et al*. [15], pseudo-anatomic landmarks were defined on the THOR-50M-RS using the average location of the anatomic landmarks from the three PMHS. This allows for comparison of the motion of the two occupant types. Kinematic plots for the THOR-50M-RS in the results section use the pseudo-anatomic landmarks for T1, T8, and L2. The definitions of the head (centre of gravity) and pelvis (H-Point) were the same for both occupants, therefore plots of the head and pelvis are not based on pseudo-anatomic landmarks.

III. RESULTS

Overall occupant motion was similar between THOR-50M-RS and PMHS (Fig. 3). As expected with a frontal impact, the occupants flex forward and the forward motion of the occupant was arrested by the shoulder belt, followed by pay out from the integrated force limiter.

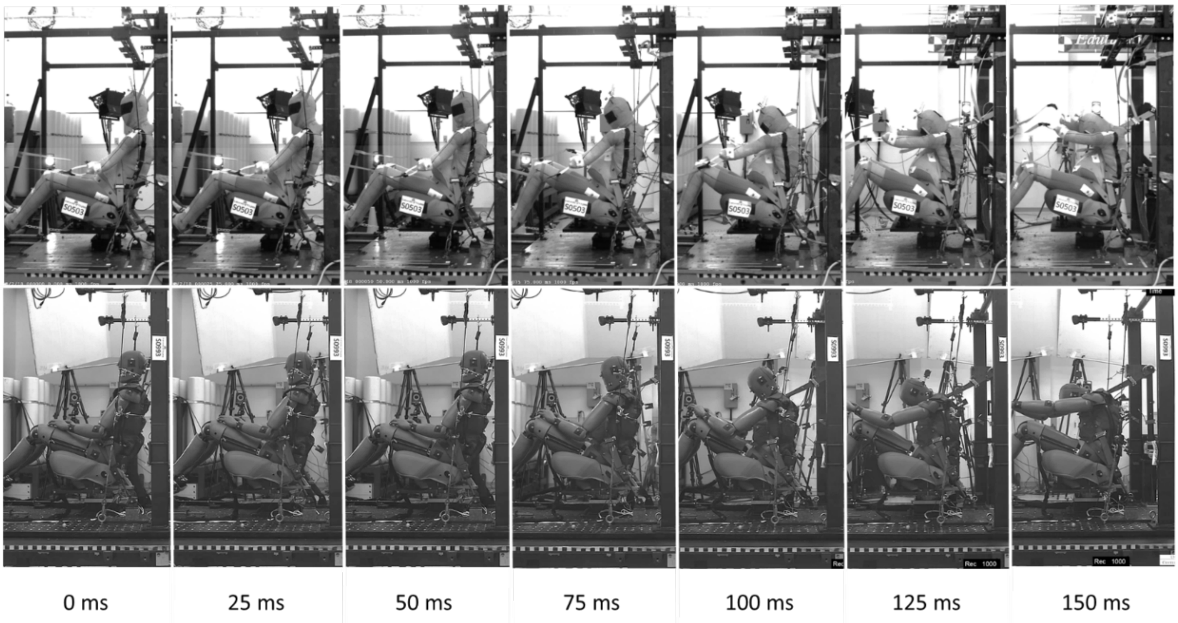

Fig. 3. High-speed video stills from time zero until 150 ms. Top: PMHS stills from S0503. Bottom: THOR-50M-RS stills from S0993.

Seat-belt forces were measured at the upper (Fig. 4) and lower (Fig. 5) shoulder belt and at the outboard lap belt (Fig. 6). The initial peak in all the time histories for both the THOR-50M-RS and the PMHS is the firing of the retractor pretensioner 10 ms after the start of the test. The plateau in shoulder-belt force after 60 ms indicates that the force-limiter in the retractor has been engaged. In the case of the THOR-50M-RS, the shoulder belt slipped off the shoulder and into the space between the shoulder pad and the neck in all three tests between 60 ms and 70 ms (identified by high-speed video). Lap-belt forces show good engagement of the pelvis by the lap belt (Fig. 6) corroborated by anterior superior iliac spine (ASIS) Force X and Moment Y (Appendix B). Moment Y readings indicate the lap belt is loading the upper portion of the ASIS. Payout of the belt was measured as vertical displacement of the motion tracking marker on the portion of the belt between the D-Ring and retractor (Fig.7). Positive displacement is pay in to the retractor upon pre-tensioning. Negative displacement is pay out of the belt by the force limiter during the impact. The retractor pre-tensioner caused more belt pay in for the THOR-50M-RS than for the PMHS. The PMHS experienced more pay out of the belt (approximately 25-36 mm) compared to the THOR-50M-RS (approximately 15-18 mm).

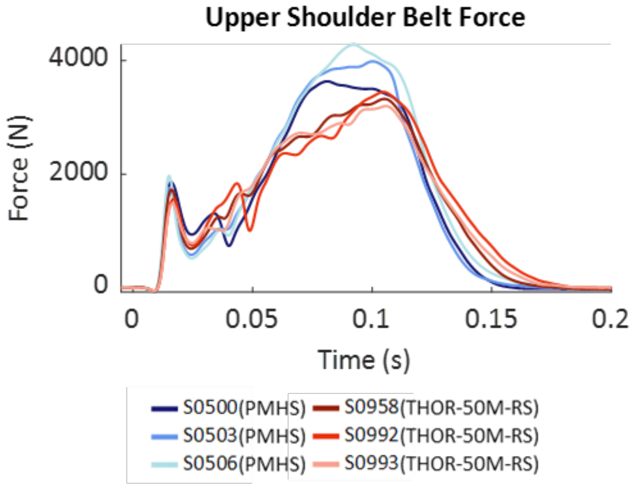

Fig. 4. Upper shoulder-belt force measured by a seat-belt load cell between the occupant shoulder and D-Ring. Data traces filtered at CFC60.

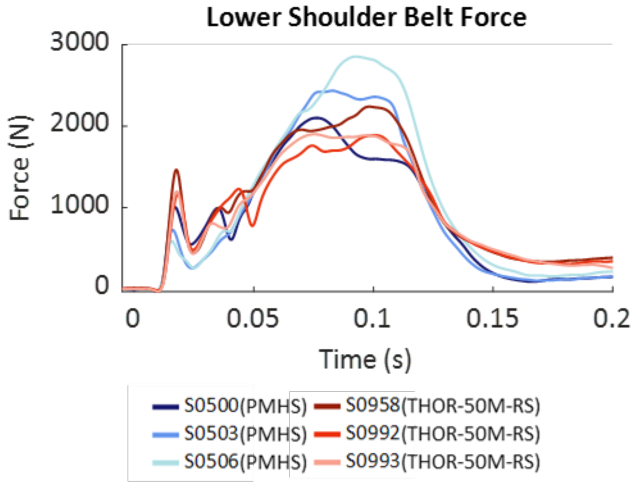

Fig. 5. Lower shoulder-belt force measured by a seat-belt load cell on the lower portion of the shoulder belt above the buckle. Data traces filtered at CFC60.

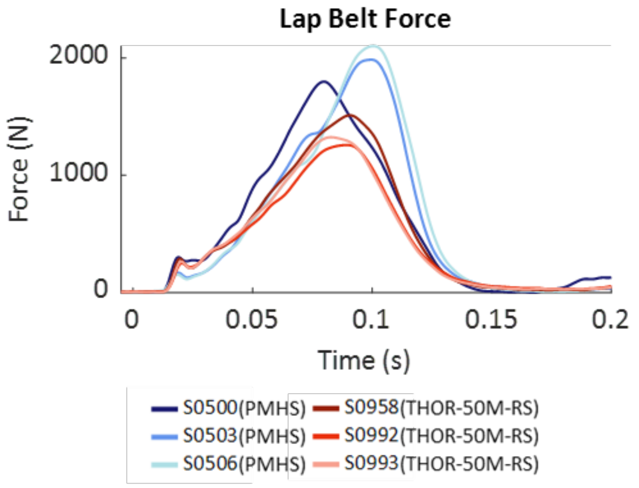

Fig. 6. Lap-belt force measured by a seat-belt load cell between the hip and lap-belt anchor. Data traces filtered at CFC60.

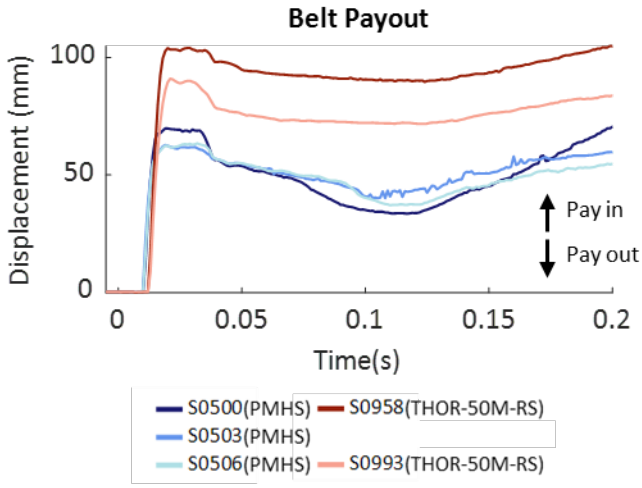

Fig. 7. Payout of the belt measured as Z-direction displacement before the D-Ring.

Motion of all the measured locations was generally consistent between the ATD and PMHS (Fig. 8). The head and spine locations all move forward and downward, with the head of the ATD travelling both farther forward and downward. The pelvis motion of the ATD in the mid-plane is generally straight forward with minimal Z motion, while the PMHS exhibit more downward displacement during the impact.

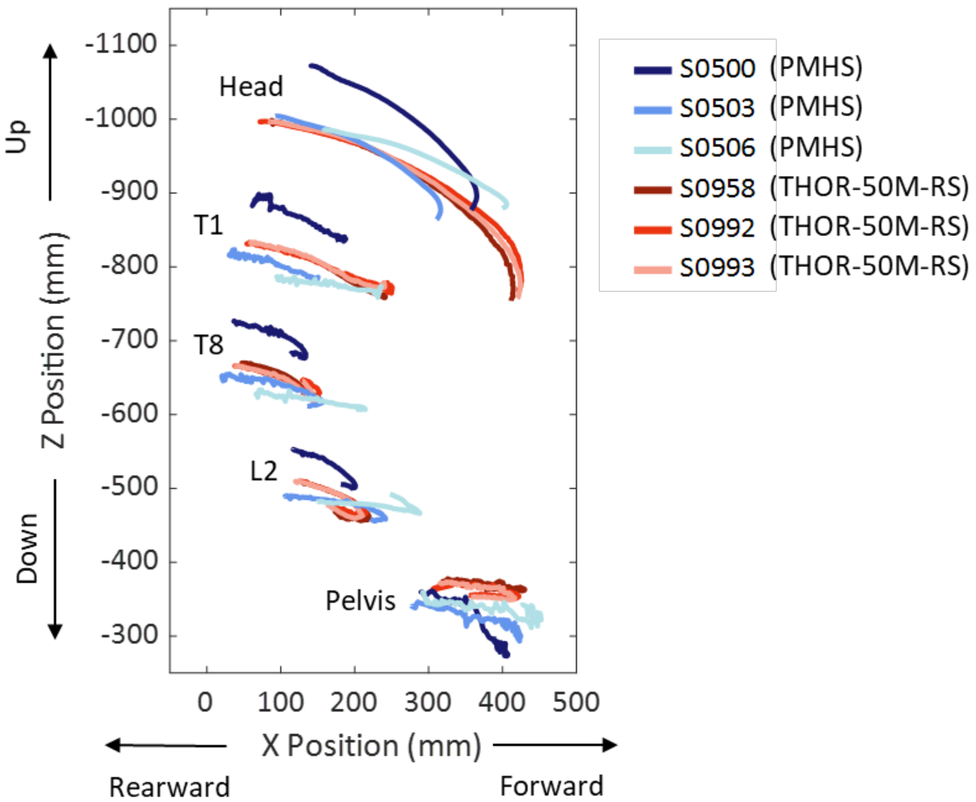

Fig. 8. Mid-plane (XZ-plane) trajectories of the THOR-50M-RS pseudo-anatomic landmarks and PMHS anatomic landmarks. Trajectories terminate just past the time of peak forward head excursion.

The head and pelvis displacements further highlight the differences in motion at those two anatomical locations (Fig. 9 and Fig. 10). For the head X and Z displacement is consistent throughout approximately 80 ms between the THOR-50M-RS and PMHS. The displacement of the pelvis is consistent through approximately 50 ms in both the X and Z directions.

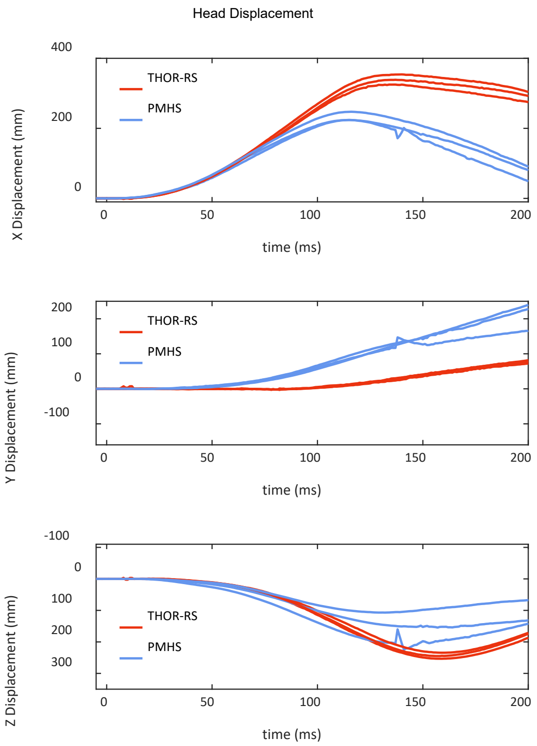

Fig. 9. Head displacement of the THOR-50M-RS compared to the 50th percentile male PMHS.

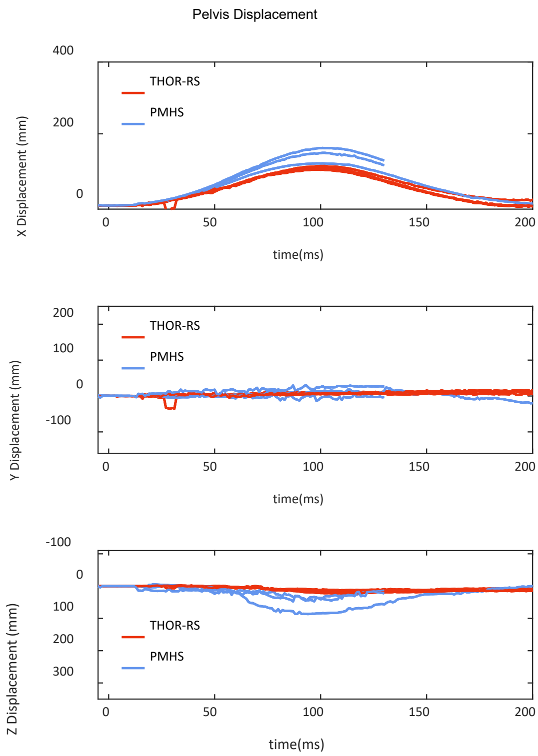

Fig. 10. Pelvis displacement of the THOR-50M-RS compared to the 50th percentile male PMHS.

Pelvis pitch (rotation about the Y-axis) differed between ATD and PMHS (Fig. 11). For the THOR-50M-RS, the pelvis rotated rearward and maximum pelvis pitch occurred after the time of maximum lap-belt force and near the time of maximum forward pelvis displacement. For the PMHS, the pelvis rotation varied between individual PMHS, with a general trend of slightly forward rotation throughout the impact.

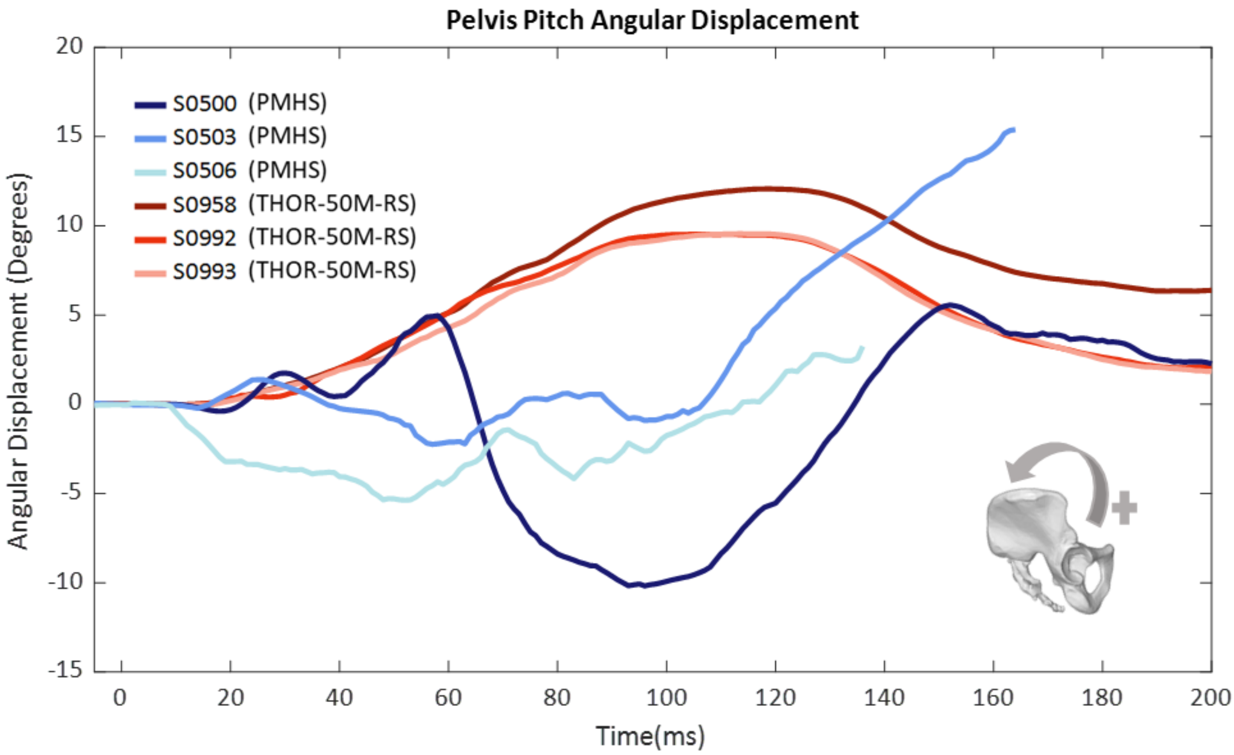

Fig. 11. Pelvis pitch angular displacement calculated from VICON motion-tracking data. Data captured at 1,000 Hz and plotted with a 10-frame moving average.

IV. DISCUSSION

Causes of Restraint Interaction Differences between PMHS and ATD

The THOR-50M-RS experienced more rearward rotation of the pelvis than the PMHS. The pelvises of the PMHS in S0503 and S0506 rotated forward, and this behaviour was not seen in the THOR-50M-RS tests. Additionally, S0500 experienced rearward rotation, similar to the THOR-50M-RS prior to submarining at 40 ms, whereafter the pelvis rotated forward. For all three PMHS, rearward rotation of the pelvis after the initial or (in the case of S0500) submarined forward rotation occurred after the time of maximum lap-belt force. There was no evidence of submarining in any of the tests with the THOR-50M-RS, as identified by high-speed video and corroborated by ASIS force and moment (Appendix B). One of the three PMHS tests experienced asymmetrical submarining, indicated by the decrease in lower shoulder-belt force (Fig. 5) at approximately 40 ms in test S0500. Despite similar downturns in lower shoulder-belt force for the THOR-50M-RS, the lap belt remained engaged with the pelvis flesh throughout the impact, as shown by the ATD lap-belt force. Despite differences in lap-belt engagement, the forces measured by the seat load cell were comparable between the PMHS and THOR-50M-RS (Appendix C). The case of submarining (S0500) is further evidenced by the downward displacement of the pelvis and deviation from the kinematic trend of the others (Fig. 8). The displacements in X, Y, and Z for the head and pelvis are shown in Fig. 9 and Fig. 10. The response of the THOR-50M-RS is similar across all three tests, suggesting strong repeatability of the ATD's performance in this condition. This is consistent with previously published tests with the THOR-50M-RS, where test to test variability was small in recline conditions [11] and an upright condition [16]. Despite differences in pelvis motion, however, the whole-body motion sequence of the 50th percentile male PMHS and the THOR-50M-RS is generally similar.

Biofidelic performance of ATD pelvises is imperative for proper pelvis restraint assessment. Previous tests of the THOR-50M in biofidelity conditions, like the Gold Standard 1, 2, and 3 conditions, limited the motion of the pelvis all together, making it hard to draw conclusions about the motion of the pelvis because it was not considered in whole-body biofidelity analysis [2]. Tests in an upright, vehicle-like environment with the THOR-50M compared to matched PMHS test exhibited similar excursions of the pelvis and observed some differences in magnitude of angular velocity depending on restraint condition, but the pelvises of the PMHS and THOR-50M rotated in the same direction (forward) [6]. The difference in pelvis rotation direction seen in this study has been observed before in tests with the THOR-50M in recline, wherein the PMHS pelvises rotated forward, while the THOR-50M rotated rearward [7]. The modifications made to the pelvis of the THOR-50M as part of the development of the THOR-50M-RS were guided in part by this observation [10,11]. In reclined frontal sled tests with a semi-rigid seat, the THOR-50M-RS experienced the same direction (forward) but lower magnitude of pelvis pitch rotation as the PMHS [11]. This highlights the potential challenge of designing an ATD that is usable across a range of postures. Despite these challenges, this goal is still worthwhile. As there is no singular definition of "reclined", development of an ATD that is only intended for use in one posture is very limiting, and would only prompt further iterations of development and modification whenever seeking to evaluate a seat design that results in a different recline angle.

Similar to the lap belt, the upper and lower shoulder-belt forces (Fig. 4 and Fig. 5) indicate different restraint interaction for the THOR-50M-RS and the PMHS. In the case of the THOR-50M-RS, the shoulder belt slipped off the shoulder and into the space between the neck assembly and shoulder cover in all three tests between 60 ms and 70 ms (Appendix D. Fig.D1). This shoulder-belt slippage and entrapment has been noted and evaluated before and is a known issue of the THOR-50M [17]. The slippage of the belt into the neck does not seemingly have a strong effect on measured shoulder-belt force between 60 and 70 ms, but there are some downturns in force that are observed in the time histories. This is likely due to seat-belt webbing slipping within the spool of the retractor, causing small decreases in force within the belt.

The nominal force limit of the shoulder belt appears to vary among PMHS and between the PMHS and THOR-50M-RS. There is a difference in both pay in and pay out of the belt between the PMHS and THOR-50M-RS (Fig.7). Anterior view high speed videos show the shoulder belt sliding along the surface of the ATD jacket in tests with the THOR-50M-RS (Appendix D. Fig. 1D). For the PMHS, the anterior view shows more pocketing of the shoulder belt into the flesh with far less sliding over the surface of the subject and therefore pay in upon pre-tensioning (Appendix D. Fig. 2D). The THOR-50M-RS also slides along the belt more throughout the impact which likely contributes to the difference in upper shoulder belt force (Fig. 4). The belt movement along the smooth surface of the jacket led to a later time of peak shoulder belt force for the THOR-50M-RS. Corresponding to later peaks in force, the shoulder belt's integrated force limiter was engaged less for the THOR-50M-RS resulting in the observed lower magnitudes of payout. The shoulder belt interaction with the material surface of the different occupant types impacted belt forces and payout. Additionally, variation among PMHS in shoulder-belt behaviour may occur due to anthropometric differences even among nominally 50th percentile PMHS, while differences between PMHS and ATDs in force-limiter behaviour may be caused by differences in the amount of seat-belt webbing drawn into the retractor by the pre-tensioner.

Future Work & Limitations

To the knowledge of the authors, this is the first study of its kind to evaluate the performance of the THOR-50M-RS in an upright frontal sled impact with real vehicle components compared to PMHS. This testing and analysis of the THOR-50M-RS was part of an ongoing analysis of the THOR-50M-RS in upright conditions across a range of simplification levels (Gold Standard 1, Gold Standard 2, Gold Standard 3, etc.). Comparison of the THOR-50M-RS to the THOR-50M can also aid in identifying additional modifications to the ATD that may improve its usability and predicative capability for assessment of automotive safety systems and increase confidence in ATD biofidelity. The results of this study are limited in their application to other types of anthropometry due to the subjects being 50th percentile male subjects. Additionally, for kinematic analysis, the test environment for the impacts was simplified and does not fully translate to a real vehicle environment. The feet were constrained, which doesn't match a real vehicle environment. This was originally done in the PMHS tests to help reduce rebound of the PMHS, since multiple tests were done on each PMHS. There might be a difference in knee torque between PMHS and THOR, but the leg angle was likely steep enough that constraint of the feet minimally affected pelvis motion. The restraint configuration in this study does not include traditional restraint structures that are commonly in front of the occupants, like air bags, steering wheels, or knee bolsters. If such structures were present, then the forward kinematics of the ATDs would likely be different. The differences in forward motion may decrease, but may translate into different degrees of engagement with the forward restraint system components. Future work should investigate the kinematic behavior of the THOR-50M-RS in a restraint configuration that includes frontal restraints beyond the seat belt to explore the effect of the observations in this study on restraint interaction.

V. CONCLUSION

The present study compared the THOR-50M-RS to mid-size male PMHS in sled tests in an upright frontal impact test with a production seat and seat belt. The use of a production seat and seat belt in an upright frontal condition highlights unique considerations for biofidelity assessment of ATDs, particularly in the interactions of the ATD with the shoulder belt (affecting head motion) and lap belt and seat (affecting pelvis displacement and rotation). The THOR-50M-RS experienced more forward head displacement and rearward pelvis rotation, while the PMHS experienced more pelvis displacement and forward rotation of the pelvis. Compared to mid-size male PMHS, the THOR-50M-RS had a similar overall kinematic response, with some differences in belt forces, shoulder belt engagement, and pelvis rotation.

VI. ACKNOWLEDGEMENTS

The authors would like to thank everyone at the University of Virginia Center for Applied Biomechanics (Charlottesville, Virginia, USA) who assisted with this project. The US Department of Transportation National Highway Traffic Safety Administration provided both technical and financial support via Contract No. 693JJ923F000288. The opinions, findings, and conclusions expressed in this publication are those of the authors and not necessarily those of the Department of Transportation or the National Highway Traffic Safety Administration. The United States Government assumes no liability for its contents or use thereof.

VII. REFERENCES

[1] Mertz, H., Irwin, A. (2014) Anthropomorphic Test Devices and Injury Risk Assessments. *Accidental Injury,* pp. 83–112. *Springer*, New York, NY, USA.

[2] Parent, D., Craig, M., Moorhouse, K. (2017) Biofidelity Evaluation of the THOR and Hybrid III 50th Percentile Male Frontal Impact Anthropomorphic Test Devices. *61st Stapp Car Crash Conference,* 2017, Charleston, South Carolina, USA.

[3] Shaw, G., Parent, D., *et al*. (2009) Impact Response of Restrained PMHS in Frontal Sled Tests: Skeletal Deformation Patterns Under Seat Belt Loading. *Stapp Car Crash Journal*, **53**: pp. 1–48.

[4] Shaw, G., Lessley, D., Ash, J., Crandall, J. (2014) Development of an Alternative Frontal Impact Condition to Assess Thoracic Response Using the THOR Mod Kit Dummy. *International Journal of Automotive Engineering*, **5**: pp. 39–46.

[5] Montesinos Acosta, S., Ash, J., *et al*. (2016) Comparison of Whole Body Response in Oblique and Full Frontal Sled Tests. *Proceedings of the IRCOBI Conference*, 2016, Florence, Italy.

[6] Albert, D., Beeman, S., Kemper, A. (2018) Occupant Kinematics of the Hybrid III, THOR-M, and Postmortem Human Surrogates Under Various Restraint Conditions in Full Scale Frontal Sled Tests. *Traffic Injury Prevention*, **19**(S1): pp. S50–58.

[7] Shin, J., Donlon, J. P., *et al*. (2022) Biofidelity Evaluation of the Hybrid III 50th Male and the THOR-50M in Reclined Frontal Impact Sled Tests. *Proceedings of the IRCOBI Conference*, 2022, Porto, Portugal.

[8] White, S., Salmon, J., *et al*. (2023) A Current Assessment of the THOR-50M in Rear Impacts. *Traffic Injury Prevention*, **24**(3): pp. 208–212.

[9] Adomeit, D. (1977) Evaluation methods for the biomechanical quality of restraint systems during frontal impact. *Proceedings of the 21st Stapp Car Crash Conference*, SAE, Warrendale, pp. 911–932.

[10] Dyer, W., Marshall, W., Winter, D., Forman, J. (2022) University of Virginia, THOR-50M Modifications for Reclined Seating Design Change Report, Contract No: DTNH2215D00022; Task Order No: 693JJ919F000222, NHTSA

[11] Klinich, K., Orton, N., *et al.* (2025) Evaluation of THOR-50M-RS Under Reclined Seating Conditions. *Traffic Injury Prevention*, **26**(S1): pp. s250–257.

[12] Donlon, J. P., Richardson, R., *et al.* (2020) Kinematics of Inboard-Leaning Occupants In Frontal Impacts. *Traffic Injury Prevention*, **21**(4): pp. 272–277.

[13] Society of Automotive Engineers (2014) SAE J211-1: Instrumentation for impact test – Part 1 – Electronic instrumentation.

[14] Forman, J. (2026) University of Virginia, *Evaluation of THOR-50M Modifications for Reclined Seating –*

Report D, NHTSA Biomechanics Database.
[15] Parent, D., Lessley, D., Shaw, G., Crandall, J. (2012) Identification of Anatomical Landmarks for Whole-Body Kinematic Measurement in the THOR Mod Kit Frontal Impact ATD. JSAE Annual Congress, 2012.
[16] Gallaher, M., Donlon, J. P., Hollar, R., Forman, J. (2025) Kinematics of the THOR-50M-RS in an Upright Frontal Sled Impact with a Simplified Restraint Environment. *Proceedings of the IRCOBI Conference*, 2025, Vilnius, Lithuania.
[17] Tylko, S., Tang, K., Giguere, F., Bussieres, A. (2018) Effects of Shoulder-belt Slip on the Kinetics and Kinematics of the THOR. *Proceedings of the IRCOBI Conference*, 2018, Athens, Greece.

VIII. APPENDIX

Appendix A – Test Set-up

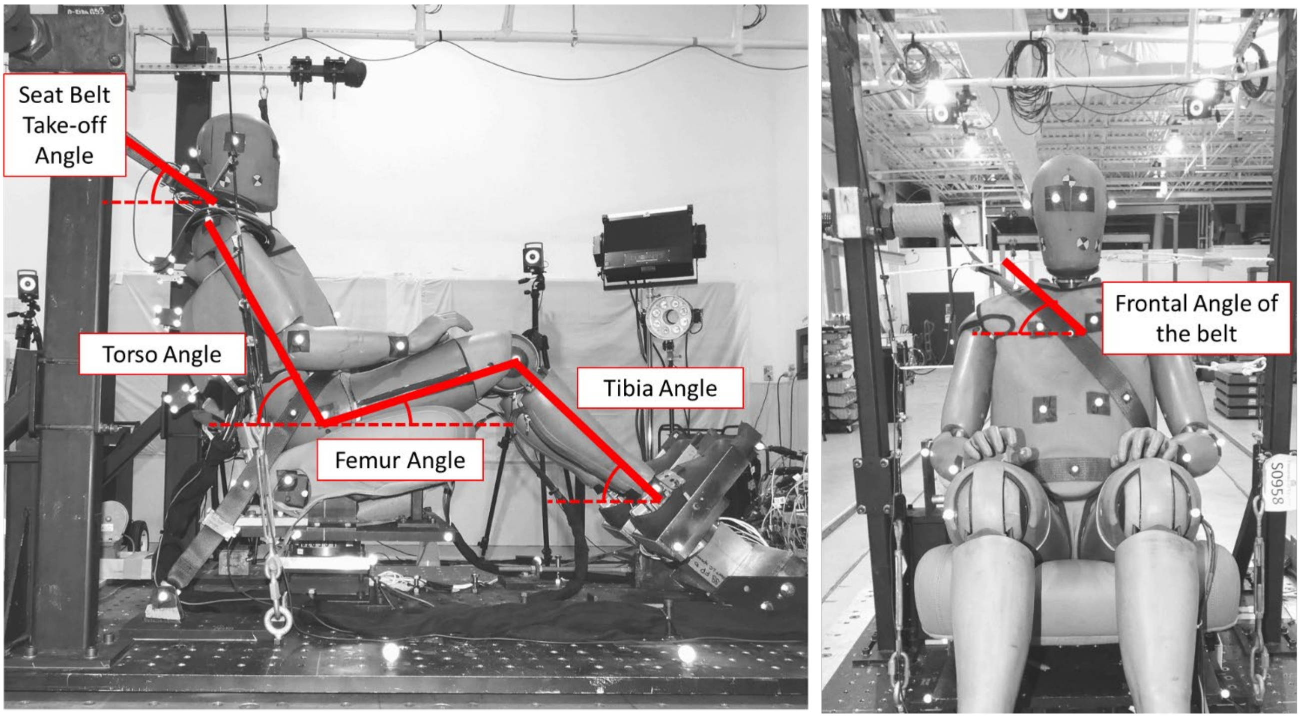

Fig. A1. Positioning Measurement Diagram.

Fig. A2. Lap Belt positioning relative to pelvis and thigh flesh.

Appendix B – ATD Data

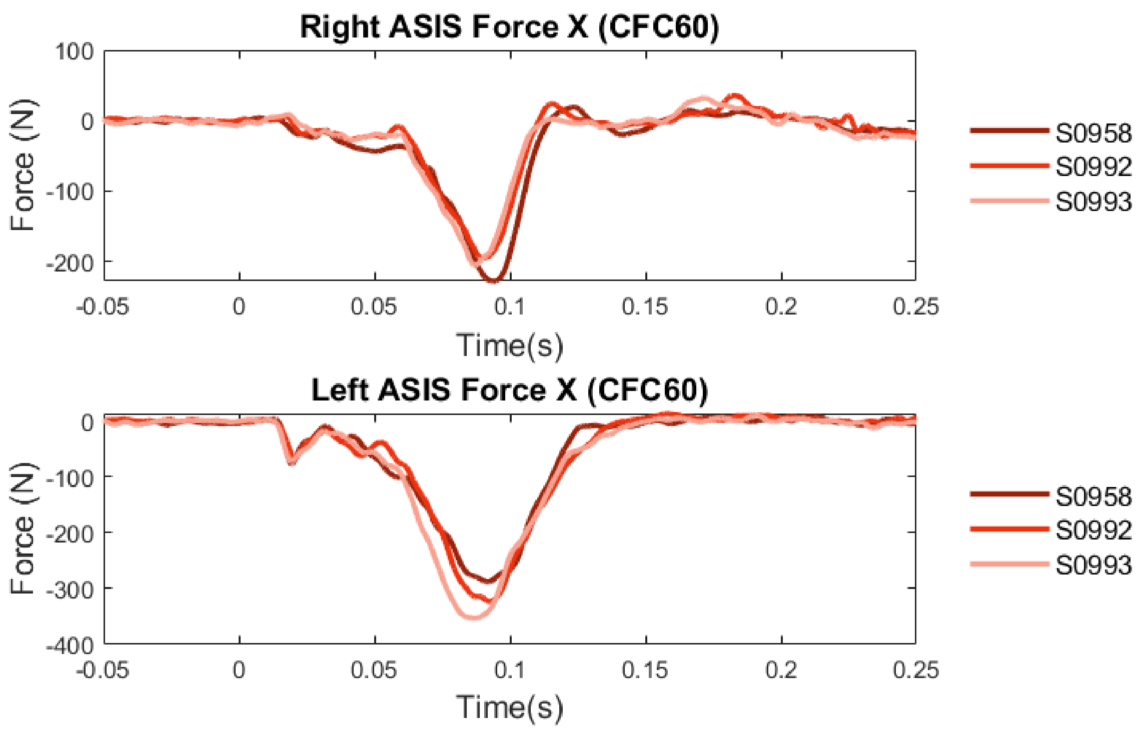

Fig. B1. ASIS right (top) and left (bottom) force X time history.

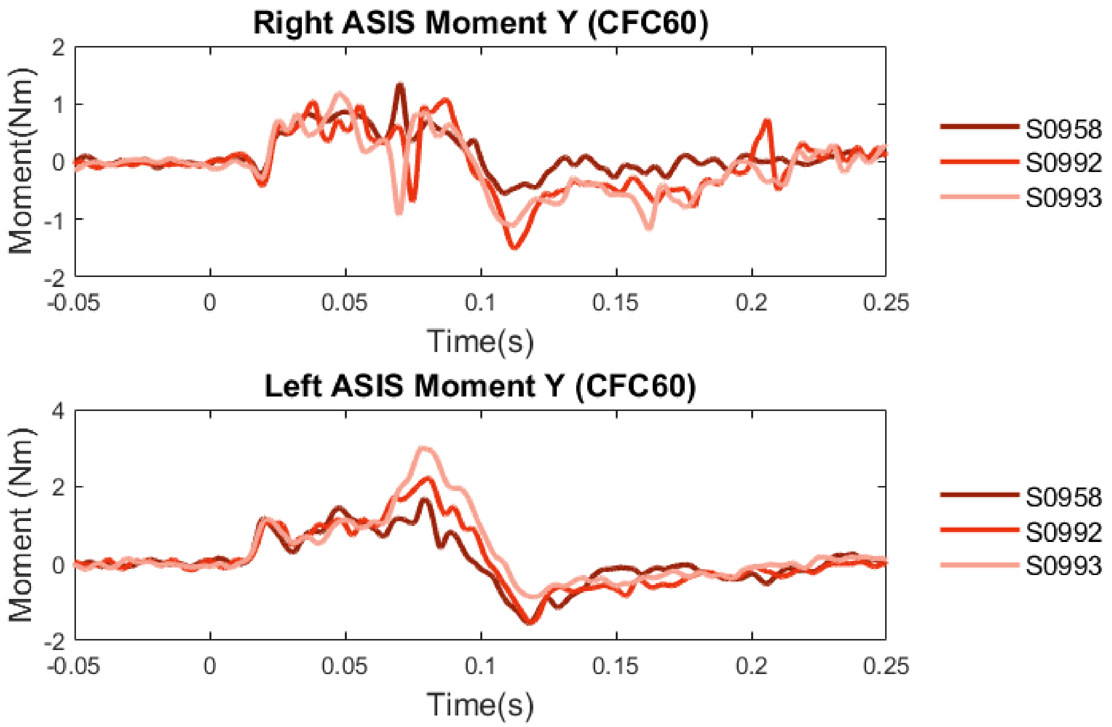

Fig. B2. ASIS right (top) and left (bottom) moment Y time history.

Appendix C – Boundary Loads

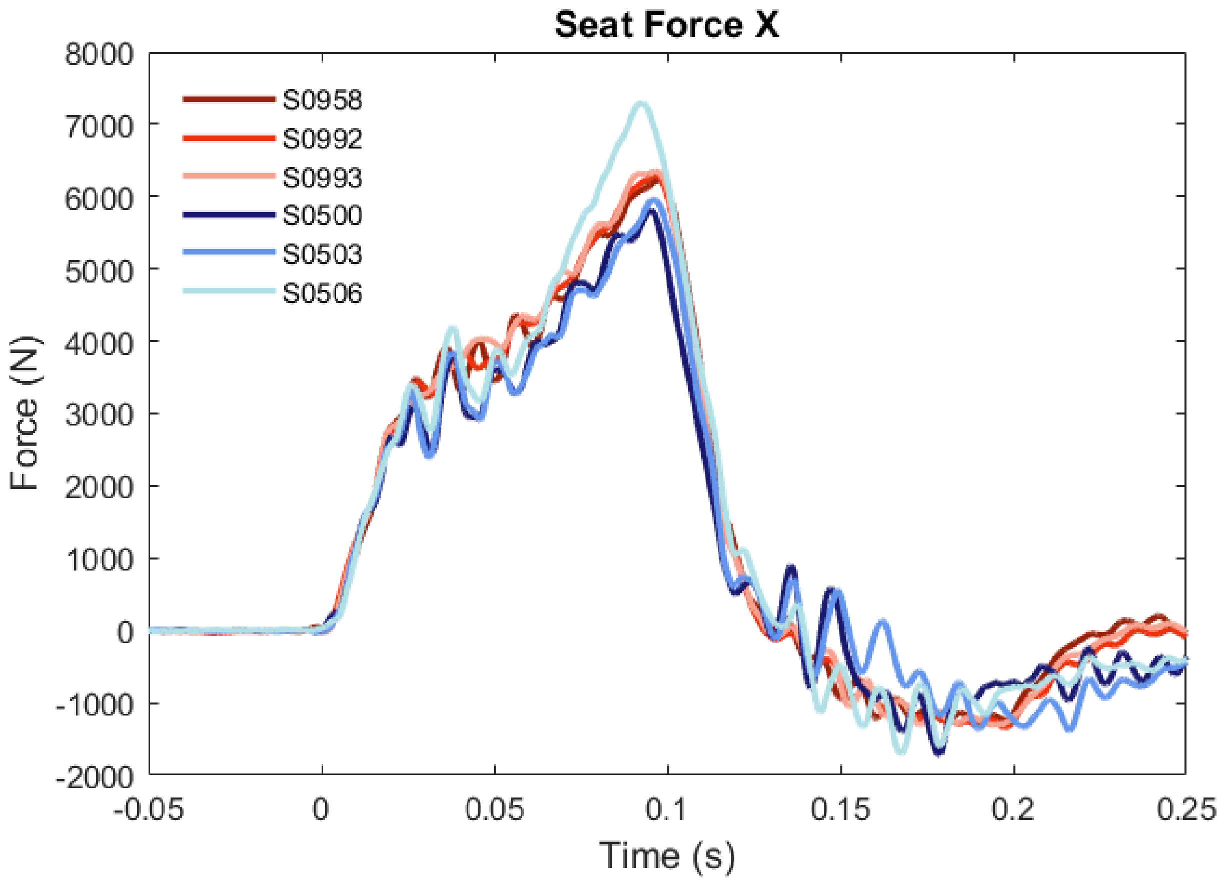

Fig. C1. Seat Force X. Filtered at CFC60.

Appendix D – Seat belt motion

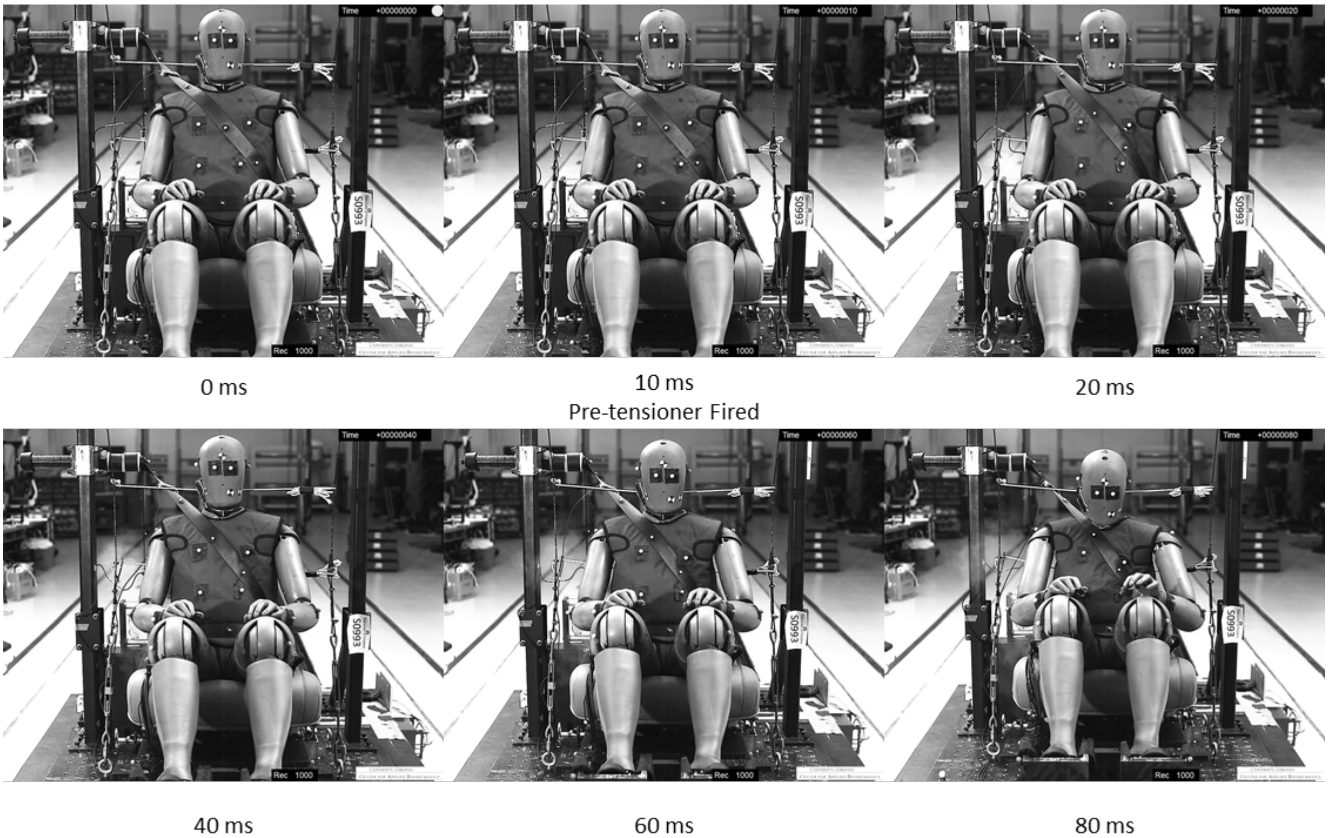

Fig. D1. Anterior view high speed video stills of the THOR-50M-RS (S0993) exhibiting sliding of the belt along the ATD jacket.

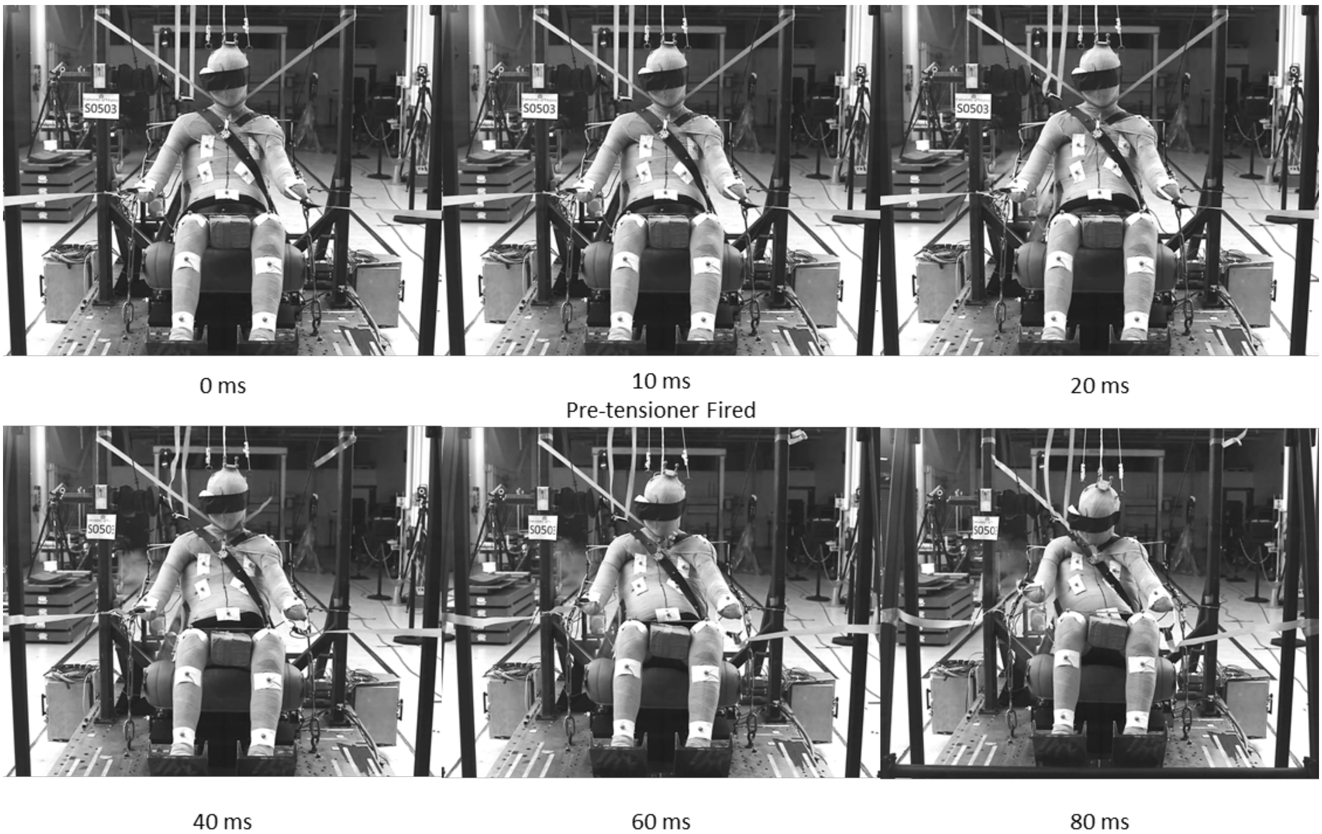

Fig. D2. Anterior view high speed video stills of PMHS (S0503) exhibiting shoulder belt motion.